

Optimizing quantum battery performance by reducing battery influence in charging dynamics

Rohit Kumar Shukla,^{1,*} Rajiv Kumar,^{2,†} Ujjwal Sen,^{3,‡} and Sunil K. Mishra^{2,§}

¹*Department of Chemistry; Institute of Nanotechnology and Advanced Materials; Center for Quantum Entanglement Science and Technology, Bar-Ilan University, Ramat-Gan, 5290002, Israel*

²*Department of Physics, Indian Institute of Technology (Banaras Hindu University) Varanasi - 221005, India*

³*Harish-Chandra Research Institute, A CI of Homi Bhabha National Institute, Chhatnag Road, Jhunsi, Prayagraj 211019, India*

Quantum batteries have emerged as promising devices that work within the quantum regime and provide energy storage and power delivery. We investigate the interplay between the battery and charger Hamiltonians, with a particular focus on *minimizing the battery's influence* during the charging dynamics. To achieve this, we introduce a control parameter that allows us to suppress the battery's contribution during the charging dynamics. We explore various configurations, including a non-interacting many-body battery with an interacting many-body charger, an interacting battery with a non-interacting charger, and systems where both the battery and charger are interacting many-body systems. Our results reveal a notable enhancement in stored energy and charging power when the battery's influence is suppressed, underscoring the pivotal role of the charger in optimizing performance. Remarkably, across all scenarios, we observe that the presence of the battery's countereffect within the charger Hamiltonian consistently leads to improved storage characteristics, highlighting a fresh direction in designing efficient quantum batteries.

I. INTRODUCTION

A quantum battery is a device designed to harness quantum properties to improve the efficiency of energy storage and retrieval. Traditional batteries store energy in chemical reactions [1–5], while quantum batteries would utilize the principles of quantum mechanics to store and release energy in a more efficient and potentially higher-capacity manner [6–13]. The basic idea behind a quantum battery is that quantum systems can exist in superposition states, meaning they can be in a combination of multiple states simultaneously. This property could potentially allow quantum batteries to store energy in a more distributed and efficient way compared to traditional batteries. Additionally, quantum entanglement, where particles become correlated in such a way that the state of one particle determines the state of the other particle, might enable quantum batteries to further enhance their energy storage capacity.

Quantum batteries have attracted significant attention in recent years [6–21]. The primary goal of these efforts is to demonstrate how quantum mechanical systems and operations can enhance the stored energy or charging power of a battery. A variety of approaches—ranging from single-qubit protocols to many-body systems—have been explored to showcase this quantum advantage [8, 10, 16, 19, 20, 22, 23]. Notable models include the Dicke quantum battery, which achieves modest speedups due to collective effects [16, 17], and qubit-based schemes

that demonstrate an N -fold power advantage, pointing to strong scalability [8]. Moreover, coherent quantum charging protocols have shown superior performance compared to classical strategies, with significantly enhanced power and robustness against decoherence and loss [24]. Recent studies have also underscored the importance of interaction topology: optimal performance in fermionic systems is observed when the interaction connectivity aligns with the interaction order [23]. In addition, alternative charging mechanisms such as those based on the Jaynes–Cummings model reveal that non-Gaussian cavity states can minimize energy fluctuations and achieve near-perfect charging fidelity [25]. These theoretical developments have been paralleled by experimental advances, with successful realizations using superconducting circuits and trapped ions [26–29]. Periodic modulation techniques have also been applied to spin systems for efficient charging [30], and the role of dissipation in open quantum systems has been investigated as a tool for enhancing performance [12, 31–38]. Notably, global charging methods—where all cells are charged simultaneously—have been shown to offer the strongest quantum advantage, with power scaling quadratically with the system size [21].

There has been a lack of discussion on the combined effect of the battery and charger in the charging dynamics, particularly in the context of spin systems. Addressing this gap, our study explores the interplay between the battery and charger during the charging process, emphasizing their joint influence on energy storage and power output. Our objective is to understand how optimizing their interactions can enhance overall performance while overcoming inherent limitations in the battery's contribution.

In quantum spin systems, both the battery and the

* rohitkrshukla.rs.phy17@itbhu.ac.in

† rajivkumar.rs.phy22@itbhu.ac.in

‡ ujjwal@hri.res.in

§ sunilkrm.app@iitbhu.ac.in

charger play a role in charging dynamics for storing energy and power. However, we observe that the battery's ability to achieve maximum storage energy and power is often constrained by the charger, which diminishes the battery's effect during the charging process. To address this, we propose introducing an additional term in the charger Hamiltonian to counteract this limitation. By incorporating the battery's countereffect into the charger, we enhance both storage energy and power across all considered configurations. This approach shifts the primary responsibility for energy storage to the charger, allowing the battery to adopt a more passive role, thereby optimizing the charging process and maximizing the efficiency of quantum batteries.

The manuscript is organized as follows: Section II introduces the setup involving the combined battery and charger system and defines the key physical quantities used in the analysis. Section III presents the results of energy storage and power calculations. Specifically, Subsection III A examines the scenario where the battery is non-interacting and the charger is interacting, while Subsection III B addresses the case of an interacting battery coupled to a non-interacting charger. Subsection III C explores the dynamics when both the battery and the charger are interacting. Finally, Section IV summarizes the main findings and concludes the manuscript.

II. SET-UP

A quantum battery typically comprises a finite number of quantum systems, such as spins, that can store and transfer energy at the quantum level. The charger, also a quantum system composed of spins, is designed to inject energy into the battery. The dynamics of these spin-based systems are described by their respective Hamiltonians. The battery Hamiltonian, \hat{H}_B , describes the internal energy levels and/or interactions within the battery, whereas the charger Hamiltonian, \hat{H}_C^e , encapsulates the dynamics and properties of the charger.

To initiate the charging process, the charger is connected to the battery, allowing them to interact. This interaction results in the formulation of the total charging Hamiltonian, which combines the contributions from both the battery and the charger. It is expressed as the sum of the battery Hamiltonian, \hat{H}_B , and the charger Hamiltonian, \hat{H}_C^e , capturing the dynamics of energy exchange between the two systems. Mathematically, it is expressed as

$$\hat{H} = \hat{H}_B + \hat{H}_C^e. \quad (1)$$

To extend the formulation, we treat the charger Hamiltonian in a unique way by considering both interacting and non-interacting forms. In each case, we incorporate the countereffect of the battery into the charger Hamiltonian to account for the mutual influence between the battery and charger during the charging dynamics. The

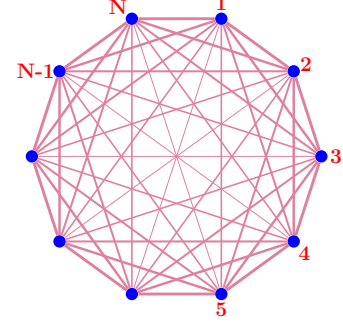


Figure 1. Illustration of all-to-all interaction of spins.

strength of this countereffect is controlled by a parameter, λ , referred to as the battery's countereffect parameter. This modified Hamiltonian is termed the effective charger Hamiltonian, as it accounts for both the intrinsic dynamics of the charger and the influence of the battery. Mathematically, it is given as:

$$\hat{H}_C^e = \hat{H}_C - \lambda \hat{H}_B. \quad (2)$$

This effective charger Hamiltonian is introduced during the charging process, where it operates alongside the battery Hamiltonian. By incorporating the battery's countereffect into the charger dynamics, the total Hamiltonian governing the charging process is updated. Substituting the effective charger Hamiltonian into the total Hamiltonian [Eq. 1], we obtain:

$$\hat{H} = \hat{H}_B + \hat{H}_C - \lambda \hat{H}_B = \hat{H}_C + (1 - \lambda) \hat{H}_B, \quad (3)$$

Physically interesting range of λ lies between $[0, 1]$. When $\lambda = 0$, the battery fully contributes to energy storage and power during the charging process. Conversely, when $\lambda = 1$, the battery's influence is completely nullified during charging. For intermediate values of λ , the battery's effect is progressively reduced, with the extent of this reduction determined by the strength of λ .

To analyze the counter effect of the battery during the charging process, we calculate two key metrics: storage energy and power. The energy stored in the battery during the charging process is defined as:

$$\Delta E = \text{Tr}[\hat{\rho}(t)\hat{H}_B] - \text{Tr}[\hat{\rho}(0)\hat{H}_B], \quad (4)$$

where $\hat{\rho}(0) = |\psi_0\rangle\langle\psi_0|$, and $|\psi_0\rangle$ is the ground state of the battery Hamiltonian. The time evolution of the system's state is given as: $|\psi(t)\rangle = \hat{U}(t)|\psi_0\rangle$, where $\hat{U}(t) = e^{-i\hat{H}t}$ is the time-evolution operator.

The storage power quantifies the rate at which energy is transferred into the system during the charging process and is given by:

$$P = \frac{\Delta E}{T}. \quad (5)$$

Here, P represents the average power over the entire charging duration, and T denotes the total charging time.

This formulation provides a measure of how efficiently energy is accumulated, offering insight into the performance and effectiveness of the energy storage process.

III. RESULT

To evaluate the performance of the quantum battery, we compute the stored energy and charging power across three distinct scenarios. In the first scenario, the battery is modeled as a non-interacting spin system, while the charger consists of interacting spins. In the second, the battery is an interacting spin system, and the charger is non-interacting. The third configuration involves both the battery and the charger as interacting spin systems. These setups allow us to systematically explore how the battery's intrinsic properties influence the energy storage and power delivery during the charging process. We begin our analysis with the first scenario.

A. Non-interacting battery and interacting charger Hamiltonian

The non-interacting battery is modeled as a collection of spins aligned along the z -direction, with each spin having a strength h . The battery Hamiltonian is defined as:

$$\hat{H}_B = h \sum_{j=1}^N \hat{\sigma}_j^z, \quad (6)$$

where N is the total number of spins. In its spectral decomposition, the battery Hamiltonian can be expressed as:

$$\hat{H}_B = h \sum_{n=1}^{2^N} E_n |E_n\rangle \langle E_n|, \quad (7)$$

where E_n are the eigenvalues, ranging from $-N$ (ground state energy) to N (highest energy level). The total number of energy levels is 2^N , with the ground state and the highest energy state being non-degenerate. The remaining energy levels exhibit degeneracy, given by ${}^N C_l$, where $l = 1, 2, \dots, N-1$, corresponding to intermediate energy levels.

The goal of charging the battery is to transition it from the ground energy state $|E_1\rangle$ with energy $-Nh$ to the highest energy state $|E_{2^N}\rangle$ with energy Nh . The maximum storage energy ΔE_{\max} is defined as:

$$\begin{aligned} \Delta E_{\max} &= \left(\text{Tr} \left[\hat{\rho}(0) \hat{H}_B \right] \right)_{\max} - \left(\text{Tr} \left[\hat{\rho}(0) \hat{H}_B \right] \right)_{\min}, \\ &= [Nh - (-Nh)] = 2Nh. \end{aligned} \quad (8)$$

The maximum storage energy of the non-interacting battery, as described by Eq. (6), is given by $2Nh$.

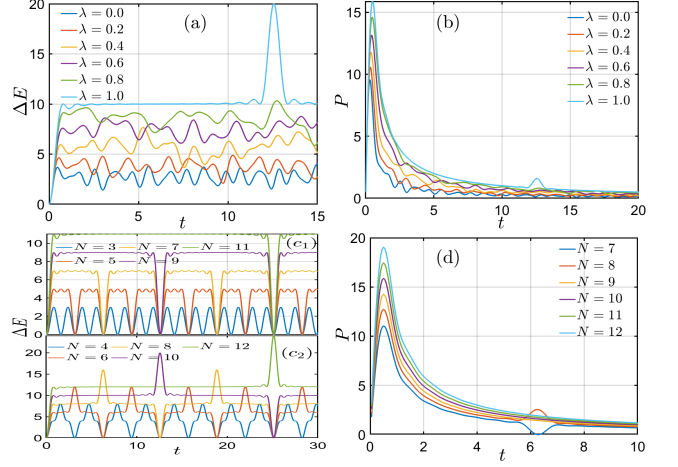


Figure 2. Non-interacting battery with ATA interacting Ising spin charger. (a) ΔE and (b) P vs. t for different values of λ with fixed system size $N = 10$. (c₁) and (c₂) show ΔE vs. t for systems with (c₁) odd and (c₂) even N with fixed $\lambda = 1$. (d) P vs. t for various N . The parameters used are $J = h = 1$, with periodic boundary conditions applied.

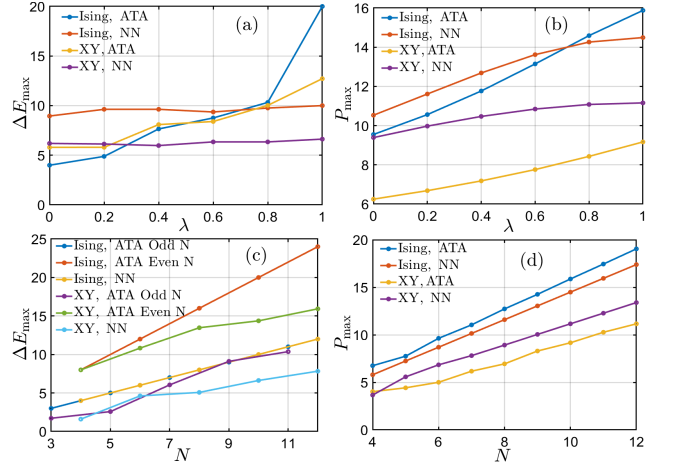


Figure 3. Maximum storage (a) energy and (b) power as functions of the battery's countereffect strength λ , for two interaction scenarios and their special cases, with system size fixed at $N = 10$. Maximum storage (c) energy and (d) power as functions of system size N , with the battery counter strength fixed at $\lambda = 1$. In all cases, the parameters used are $J = h = 1$, and $\gamma = 0.5$.

To examine the influence of the battery's countereffect on its storage energy and power, we consider an *all-to-all (ATA) interacting Ising spin system as an interacting charger*, as illustrated in Fig. 1. The interaction strength between a spin and its k -th neighbor decays as $\frac{1}{2^{k-1}}$. The corresponding Hamiltonian is given by:

$$\hat{H}_C = J \sum_{j=1}^N \left(\sum_{k=1}^{\mathcal{K}} \frac{1}{2^{k-1}} \sigma_j^x \sigma_{j+k}^x \right), \quad (9)$$

where \mathcal{K} represents the maximum interaction range. We

assume periodic boundary conditions, i.e., $\hat{\sigma}_{N+k} = \hat{\sigma}_k$, to preserve translational symmetry and eliminate edge effects. To avoid redundancy under periodic boundary conditions, we fix $\mathcal{K} = \frac{N-1}{2}$ for odd N and $\mathcal{K} = \frac{N}{2}$ for even N , ensuring that each spin pair is included only once.

We calculate the storage energy of the non-interacting battery Hamiltonian with the ATA connected Ising spin system as the charger Hamiltonian for different values of λ ranging from $[0, 1]$. It is observed that for all values of λ (except at $\lambda = 1$), the storage energy increases and eventually oscillates about a particular value with random amplitudes and frequencies. At $\lambda = 1$, the storage energy increases and saturates at a particular value. However, at a certain time, a sudden jump occurs, leading to the highest storage energy, $\Delta E_{\max} = 2hN$. This suggests that at this value of λ , the battery reaches its highest energy state [Fig. 2(a)].

The storage power exhibits a similar behavior for all values of λ , increases, reaches its maximum value at a specific time, and then starts to decrease. As the value of λ increases, the maximum storage power also increases. [Fig. 2(b)].

The storage energy is analyzed as a function of the system size, with the parameter λ fixed at 1, revealing an odd-even effect in its behaviour. For odd system sizes, the storage energy increases, saturates at a particular value with very small oscillation amplitudes, and then decreases to zero at a specific time. The region of saturation also depends on the system size. As the system size increases, the time regime of constant energy increases. In other words, the storage energy exhibits periodic behavior, with the period of the storage energy increasing as the system size grows [Fig. 2(c₁)]. Additionally, maxima of the storage energy also increase with increasing system size. Conversely, for even system sizes, the storage energy increases as time progresses, saturates for a fixed period, and reaches its maximum value at a specific time. The maximum value of the storage energy suggests that, in this scenario, the battery attains its highest energy state, $2hN$. Similar to odd system sizes, the storage energy for even system sizes also exhibits periodic behavior, with the period increasing as the system size grows [Fig. 2(c₂)].

The storage power of the battery is analyzed as a function of the system size with a fixed value of $\lambda = 1$. It is observed that while the storage power depends on the system size, it does not exhibit the odd-even effect. For all system sizes, the storage power increases over time, reaches a maximum value, and then begins to decline. The maximum storage energy increases with the growth of the system size. [Fig. 2(d)].

Optimum storage energy and power

To better understand how the counter effect influences the charging process, we investigate how the maximum

storage energy and charging power vary with the counter effect parameter λ . We also examine how these quantities scale with the system size. For this purpose, we consider two distinct types of charger Hamiltonians.

The first type is defined in Eq. (9) and corresponds to the Ising spin system with ATA interactions. As a special case, we also study the nearest-neighbor (NN) Ising spin system by setting the interaction range $\mathcal{K} = 1$. In this case, the charger Hamiltonian simplifies to the standard NN Ising model:

$$\hat{H}_C = J \sum_{j=1}^N \hat{\sigma}_j^x \hat{\sigma}_{j+1}^x. \quad (10)$$

The second type of charger is qualitatively different and is based on the XY spin system with ATA interactions. The Hamiltonian is given by:

$$\begin{aligned} \hat{H}_C = & (1 + \gamma) \sum_{j=1}^N \left(\sum_{k=1}^{\mathcal{K}} \frac{1}{2^{k-1}} \hat{\sigma}_j^x \hat{\sigma}_{j+k}^x \right) \\ & + (1 - \gamma) \sum_{j=1}^N \left(\sum_{k=1}^{\mathcal{K}} \frac{1}{2^{k-1}} \hat{\sigma}_j^y \hat{\sigma}_{j+k}^y \right), \end{aligned} \quad (11)$$

where γ is the anisotropy parameter and \mathcal{K} denotes the interaction range. We also consider the NN case of the Eq. (11) that is obtained by setting $\mathcal{K} = 1$, resulting in the following Hamiltonian:

$$\hat{H}_C = (1 + \gamma) \sum_{j=1}^N \hat{\sigma}_j^x \hat{\sigma}_{j+1}^x + (1 - \gamma) \sum_{j=1}^N \hat{\sigma}_j^y \hat{\sigma}_{j+1}^y. \quad (12)$$

By analyzing these different charger configurations, we systematically compare their influence on the battery's maximum storage energy and power. This comparison provides valuable insights into how the type and range of interactions affect the performance and optimization of quantum batteries.

By employing two types of charger Hamiltonians—Ising and XY models—with both ATA interactions and their special case of NN interactions, we investigate the maximum storage energy and power of the battery as functions of the countereffect strength and the system size.

In all considered cases, the maximum storage energy increases with increasing λ and reaches its optimum at $\lambda = 1$. [Fig. 3(a)]. For the Ising spin system with ATA interactions, the maximum storage energy reaches the upper bound of $2hN$ at $\lambda = 1$. In contrast, when restricted to NN interactions, the storage energy only reaches half this value, i.e., hN , at the same λ . In the case of the XY ATA interacting charger, the battery attains a maximum storage energy greater than hN , though not reaching $2hN$. For the XY NN case, the energy remains below hN even at $\lambda = 1$. These observations highlight that long-range interactions (especially ATA) significantly enhance the energy storage capacity of the quantum battery. Thus, $\lambda = 1$ marks an optimal point where energy

transfer during the charging protocol becomes most efficient, particularly in systems with long-range interactions.

The behavior of the storage power also supports the efficiency of the charging protocol with increasing countereffect. As shown in Fig. 3(b), the maximum storage power increases approximately linearly with λ in all the considered cases, reaching its optimum value at $\lambda = 1$. These results reinforce the conclusion that the countereffect of the battery—modeled by the parameter λ —facilitates more efficient energy transfer and charging dynamics. In particular, $\lambda = 1$ consistently yields the best performance in terms of both storage energy and power across all interacting charger configurations. Among the different interaction types, the Ising spin systems (both NN and ATA) exhibit higher storage power compared to their XY counterparts. This indicates that the nature of the spin-spin interaction affects the storage capacity.

Furthermore, we investigate how the system size N influences the maximum storage energy and power, keeping the countereffect parameter fixed at $\lambda = 1$. Interestingly, for chargers with ATA interactions, we observe an *odd-even effect* in the storage energy behavior. In the Ising ATA case, when the system size N is even, the maximum storage energy reaches its upper bound of $2hN$, whereas for odd N , it only attains half of that value, i.e., hN . On the other hand, in the NN Ising interaction case, the storage energy consistently reaches half of the maximum possible value, hN , regardless of system size. A similar odd-even behavior appears in the XY ATA interacting charger. For odd system sizes, the storage energy remains below half of the maximum value ($< hN$), while for even system sizes, it exceeds half the maximum ($> hN$). In contrast, the XY NN configuration yields a storage energy that remains below hN for all system sizes [Fig. 3(c)].

The storage power exhibits a linear increase with system size N across all the considered charger configurations. Among them, the Ising ATA interaction yields the highest storage power, demonstrating superior charging efficiency. In contrast, the XY ATA configuration results in the lowest storage power, indicating relatively less efficient energy transfer dynamics [Fig. 3(d)].

B. Interacting battery and non-interacting charger Hamiltonian

To generalize our observation that the countereffect of a battery in the charging dynamics enhances storage energy and power, we now consider a reversed setup: an interacting battery coupled to a non-interacting charger. The interacting battery Hamiltonians considered are of two types: *Ising spin system with NN interaction* defined by Eq.(10), i.e., $\hat{H}_B = J \sum_{j=1}^N \sigma_j^x \sigma_{j+1}^x$, and *XY spin system with NN interaction* defined by Eq.(12), i.e., $\hat{H}_B = (1 + \gamma) \sum_{j=1}^N \sigma_j^x \sigma_{j+1}^x + (1 - \gamma) \sum_{j=1}^N \sigma_j^y \sigma_{j+1}^y$. The

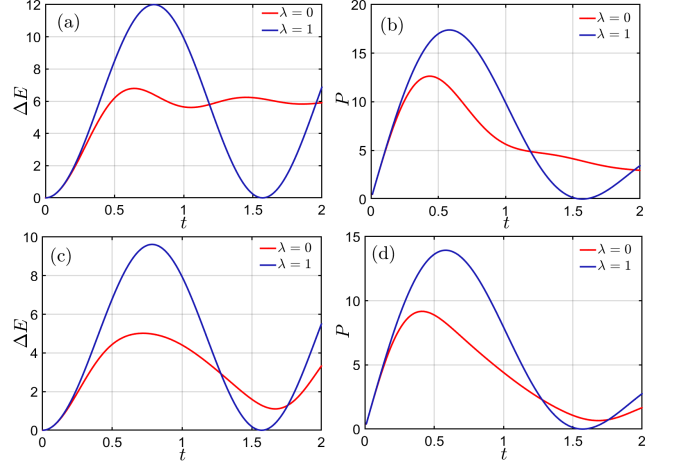


Figure 4. (a) ΔE and (b) P vs. t for NN Ising interacting Hamiltonian as a battery and non-interacting Hamiltonian as a charger. (c) ΔE and (d) P vs. t for NN interacting XY spin system as a battery and non-interacting Hamiltonian as a charger. Parameters are: $N = 12$, $J = 1$, $h = 1$, and $\gamma = 0.5$. Periodic boundary conditions are considered.

non-interacting charger Hamiltonian is given by Eq. (6), i.e., $\hat{H}_C = h \sum_{j=1}^N \hat{\sigma}_j^z$.

We analyze the storage energy and power of the battery in two scenarios: one where the battery's influence on the charger is present ($\lambda = 0$) and another where it is absent ($\lambda = 1$). The results demonstrate that, for both Ising and XY interacting batteries, storage energy and power are notably higher when $\lambda = 1$, underscoring the beneficial role of the battery's countereffect in the charging dynamics. Additionally, the Ising model consistently yields superior performance over the XY model in both metrics, as shown in Fig. 4(a-d).

C. Interacting battery and interacting charger Hamiltonian

We consider the scenario where both the battery and charger are governed by interacting Hamiltonians. First, we analyze the case where the battery is modeled by an Ising spin system with NN interactions [Eq. (10)], and the charger is described by an NN XY-interacting Hamiltonian [Eq. (12)]. We calculate the storage energy and power in two situations: when the battery's influence is present in the charging dynamics ($\lambda = 0$) and when it is absent ($\lambda = 1$). Our results indicate that the presence of the counter effect of battery during charging leads to an advantage in both the stored energy and the power [Fig. 5(a,b)].

Next, we examine the reverse configuration: the battery is now represented by an NN XY-interacting spin system [Eq. (12)], while the charger is governed by an NN Ising-type interaction [Eq. (10)]. In this case, we again compute the storage energy and power, and we

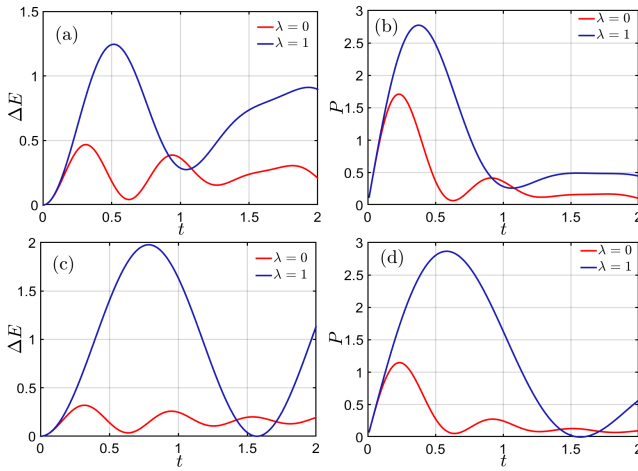


Figure 5. (a) ΔE and (b) P as a function of time t for a NN interacting Ising spin system as the battery and NN interacting XY spin system as the charger Hamiltonian. (c) ΔE and (d) P vs. t for a NN interacting XY spin system as the battery and NN interacting Ising spin system as the charger Hamiltonian. The system parameters are $N = 12$, $J = 1$, and $\gamma = 0.5$. Periodic boundary conditions are considered.

find that when the battery's influence is absent in the charging dynamics ($\lambda = 1$), the system exhibits improved performance in terms of both energy storage and power [Fig. 5(c,d)].

In nutshell, across all scenarios considered, the presence of the battery's counter effect in the charging dynamics consistently provides an advantage in both energy storage and power. This advantage is consistent for being independent of the interaction and noninteration of the battery and charger Hamiltonians.

IV. CONCLUSION

In this work, we explored the role of the battery's countereffect in the charging dynamics of quantum batteries composed of spin systems. By analyzing various configurations involving both non-interacting and interacting Hamiltonians for the battery and charger, we demon-

strated how their interplay significantly impacts storage energy and power.

We began by examining a non-interacting battery coupled to an interacting charger modeled by an ATA Ising spin system. Our results revealed that incorporating the battery's countereffect into the dynamics ($\lambda = 1$) leads to optimal performance, with the storage energy reaching its theoretical maximum $2Nh$ and the power also peaking. Notably, an odd-even parity effect emerged in energy storage for increasing system sizes, while power remained parity-independent.

To further understand the influence of interaction types and ranges, we compared Ising and XY charger models with both ATA and NN interactions. Across all these cases, the optimum storage energy and power consistently occurred at $\lambda = 1$, emphasizing the constructive role of the countereffect in enhancing energy transfer. Both quantities exhibited linear scaling with system size, confirming the scalability of our protocol.

Extending the analysis to interacting batteries with non-interacting chargers, where the battery is governed by either Ising or XY NN interactions, we observed that the inclusion of the countereffect continued to offer superior energy and power outcomes. This advantage persisted even in the most general scenario where both the battery and charger are interacting systems, reinforcing the robustness of our findings across diverse interaction frameworks.

Interestingly, in cases where the charger is modeled with ATA interactions, the charging power peaks beyond the physically meaningful range ($\lambda > 1$). Although this shift lies outside the regime of practical relevance, it suggests the presence of underlying physical mechanisms that merit deeper investigation. A detailed discussion of this anomaly is provided in Appendix A.

Altogether, our study establishes the critical importance of retaining the battery's countereffect in the charger Hamiltonian for optimizing quantum battery performance. These insights offer valuable guidance for the design of efficient and scalable quantum energy storage devices and open new avenues for exploring interaction-driven enhancements in quantum thermodynamic protocols.

[1] G. Liu, L. Lu, H. Fu, J. Hua, J. Li, M. Ouyang, Y. Wang, S. Xue, and P. Chen, A comparative study of equivalent circuit models and enhanced equivalent circuit models of lithium-ion batteries with different model structures, in *2014 IEEE Conference and Expo Transportation Electrification Asia-Pacific (ITEC Asia-Pacific)* (IEEE, 2014) pp. 1–6.

[2] H. Chaoui, C. C. Ibe-Ekeocha, and H. Gualous, Aging prediction and state of charge estimation of a lifepo4 battery using input time-delayed neural networks, *Electric Power Systems Research* **146**, 189 (2017).

[3] Z. Chen, Y. Fu, and C. C. Mi, State of charge estimation of lithium-ion batteries in electric drive vehicles using extended kalman filtering, *IEEE Transactions on Vehicular Technology* **62**, 1020 (2012).

[4] C. Fleischer, W. Waag, Z. Bai, and D. U. Sauer, Adaptive on-line state-of-available-power prediction of lithium-ion batteries, *Journal of Power Electronics* **13**, 516 (2013).

[5] J. P. Rivera-Barrera, N. Muñoz-Galeano, and H. O. Sarmiento-Maldonado, Soc estimation for lithium-ion batteries: Review and future challenges, *Electronics* **6**, 102 (2017).

[6] R. Alicki and M. Fannes, Entanglement boost for extractable work from ensembles of quantum batteries,

Physical Review E **87**, 042123 (2013).

[7] K. V. Hovhannissyan, M. Perarnau-Llobet, M. Huber, and A. Acín, Entanglement generation is not necessary for optimal work extraction, *Physical review letters* **111**, 240401 (2013).

[8] F. C. Binder, S. Vinjanampathy, K. Modi, and J. Goold, Quantacell: powerful charging of quantum batteries, *New Journal of Physics* **17**, 075015 (2015).

[9] F. Campaioli, F. A. Pollock, F. C. Binder, L. Céleri, J. Goold, S. Vinjanampathy, and K. Modi, Enhancing the charging power of quantum batteries, *Physical review letters* **118**, 150601 (2017).

[10] T. P. Le, J. Levinsen, K. Modi, M. M. Parish, and F. A. Pollock, Spin-chain model of a many-body quantum battery, *Physical Review A* **97**, 022106 (2018).

[11] S. Ghosh, T. Chanda, A. Sen, *et al.*, Enhancement in the performance of a quantum battery by ordered and disordered interactions, *Physical Review A* **101**, 032115 (2020).

[12] D. Farina, G. M. Andolina, A. Mari, M. Polini, and V. Giovannetti, Charger-mediated energy transfer for quantum batteries: An open-system approach, *Physical Review B* **99**, 035421 (2019).

[13] S. Ghosh and A. Sen(De), Dimensional enhancements in a quantum battery with imperfections, *Phys. Rev. A* **105**, 022628 (2022).

[14] X. Yang, Y.-H. Yang, M. Alimuddin, R. Salvia, S.-M. Fei, L.-M. Zhao, S. Nimmrichter, and M.-X. Luo, Battery capacity of energy-storing quantum systems, *Physical Review Letters* **131**, 030402 (2023).

[15] L. Peng, W.-B. He, S. Chesi, H.-Q. Lin, and X.-W. Guan, Lower and upper bounds of quantum battery power in multiple central spin systems, *Physical Review A* **103**, 052220 (2021).

[16] D. Ferraro, M. Campisi, G. M. Andolina, V. Pellegrini, and M. Polini, High-power collective charging of a solid-state quantum battery, *Physical review letters* **120**, 117702 (2018).

[17] G. M. Andolina, M. Keck, A. Mari, V. Giovannetti, and M. Polini, Quantum versus classical many-body batteries, *Physical Review B* **99**, 205437 (2019).

[18] N. Friis and M. Huber, Precision and work fluctuations in gaussian battery charging, *Quantum* **2**, 61 (2018).

[19] S. Julià-Farré, T. Salamon, A. Riera, M. N. Bera, and M. Lewenstein, Bounds on the capacity and power of quantum batteries, *Physical Review Research* **2**, 023113 (2020).

[20] D. Rossini, G. M. Andolina, D. Rosa, M. Carrega, and M. Polini, Quantum advantage in the charging process of sachdev-ye-kitaev batteries, *Physical Review Letters* **125**, 236402 (2020).

[21] J.-Y. Gyhm, D. Šafránek, and D. Rosa, Quantum charging advantage cannot be extensive without global operations, *Physical Review Letters* **128**, 140501 (2022).

[22] D. Rosa, D. Rossini, G. M. Andolina, M. Polini, and M. Carrega, Ultra-stable charging of fast-scrambling syk quantum batteries, *Journal of High Energy Physics* **2020**, 1 (2020).

[23] G. Francica, Quantum advantage in batteries for sachdev-ye-kitaev interactions, *Physical Review A* **110**, 062209 (2024).

[24] R. Salvia, M. Perarnau-Llobet, G. Haack, N. Brunner, and S. Nimmrichter, Quantum advantage in charging cavity and spin batteries by repeated interactions, *Physical Review Research* **5**, 013155 (2023).

[25] D. Rinaldi, R. Filip, D. Gerace, and G. Guarneri, Reliable quantum advantage in quantum battery charging, *arXiv preprint arXiv:2412.15339* (2024).

[26] J. Q. Quach, K. E. McGhee, L. Ganzer, D. M. Rouse, B. W. Lovett, E. M. Gauger, J. Keeling, G. Cerullo, D. G. Lidzey, and T. Virgili, Superabsorption in an organic microcavity: Toward a quantum battery, *Science advances* **8**, eabk3160 (2022).

[27] C.-K. Hu, J. Qiu, P. J. Souza, J. Yuan, Y. Zhou, L. Zhang, J. Chu, X. Pan, L. Hu, J. Li, *et al.*, Optimal charging of a superconducting quantum battery, *Quantum Science and Technology* **7**, 045018 (2022).

[28] F.-Q. Dou and F.-M. Yang, Superconducting transmon qubit-resonator quantum battery, *Physical Review A* **107**, 023725 (2023).

[29] J. Joshi and T. Mahesh, Experimental investigation of a quantum battery using star-topology nmr spin systems, *Physical Review A* **106**, 042601 (2022).

[30] S. Mondal and S. Bhattacharjee, Periodically driven many-body quantum battery, *Physical Review E* **105**, 044125 (2022).

[31] S. Ghosh, T. Chanda, S. Mal, A. Sen, *et al.*, Fast charging of a quantum battery assisted by noise, *Physical Review A* **104**, 032207 (2021).

[32] S.-Q. Liu, L. Wang, H. Fan, F.-L. Wu, and S.-Y. Liu, Better performance of quantum batteries in different environments compared to closed batteries, *Physical Review A* **109**, 042411 (2024).

[33] A. C. Santos, Quantum advantage of two-level batteries in the self-discharging process, *Physical Review E* **103**, 042118 (2021).

[34] S.-Y. Bai and J.-H. An, Floquet engineering to reactivate a dissipative quantum battery, *Physical Review A* **102**, 060201 (2020).

[35] J. Q. Quach and W. J. Munro, Using dark states to charge and stabilize open quantum batteries, *Physical Review Applied* **14**, 024092 (2020).

[36] M. Carrega, A. Crescente, D. Ferraro, and M. Sassetti, Dissipative dynamics of an open quantum battery, *New Journal of Physics* **22**, 083085 (2020).

[37] F. Zhao, F.-Q. Dou, and Q. Zhao, Quantum battery of interacting spins with environmental noise, *Physical Review A* **103**, 033715 (2021).

[38] F. Barra, Dissipative charging of a quantum battery, *Physical review letters* **122**, 210601 (2019).

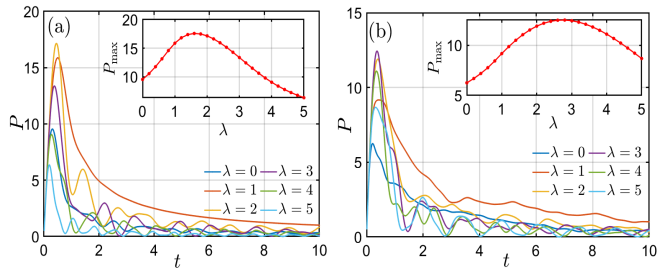


Figure 6. Storage power $P(t)$ as a function of time t for ATA interacting (a) Ising and (b) XY charger Hamiltonian, shown for various values of the countereffect parameter λ . The insets display the corresponding maximum storage power as a function of λ . Parameters used: $J = h = 1$, $N = 10$, and $\gamma = 0.5$.

Appendix A: Charging dynamics beyond physical regime

In the main manuscript, we investigate the charging dynamics of quantum batteries within the physically acceptable range of the countereffect parameter, $\lambda \in [0, 1]$. Within this regime, both the storage energy and power

attain their maximum at $\lambda = 1$. Interestingly, our analysis further reveals that the storage power reaches an even higher value beyond this physical regime ($\lambda > 1$) in the case of ATA interacting Ising and XY charger Hamiltonians. However, the storage energy still achieves its maximum at $\lambda = 1$. Although the region $\lambda > 1$ falls outside the standard physical constraints, we emphasize this result to highlight its potential implications and to encourage future investigations into such unconventional regimes.

We analyze the storage power for a non-interacting battery defined by Eq. (6) and ATA-interacting Ising and XY chargers described by Eq. (9) and Eq. (11), respectively, considering the countereffect parameter of the battery in the range $\lambda \in [0, 5]$. In both cases, for all values of λ , the storage power exhibits a consistent trend: it initially increases, reaches a maximum value, and subsequently decreases after a certain time [Fig. 6(a,b)]. The maximum storage power, P_{\max} , depends on λ and increases with it, attaining its peak at $\lambda = 1.6$ for the ATA interacting Ising charger and $\lambda = 2.8$ for the ATA interacting XY charger. Beyond these points, the storage power decreases with further increases in λ [inset of Fig. 6(a,b)]. Remarkably, the highest P_{\max} values occur outside the physically accepted regime ($\lambda > 1$).